PRAMANA
—journal of
physics

© Printed in India

Vol. 49, No. 1,
July 1997
pp. 93–107

Chaos and its implications

B BUTI
National Physical Laboratory, New Delhi 110012, India

Abstract. Starting with the very definition of chaos, we demonstrate that the study of chaos is not an abstract one but can lead to some useful practical applications. With the advent of some powerful mathematical techniques and with the availability of fast computers, it is now possible to study the fascinating phenomena of chaos – the subject which is truly interdisciplinary. The essential role played by fractals, strange attractors, Poincare maps, etc., in the study of chaotic dynamics, is briefly discussed. Phenomena of self-organization, coherence in chaos and control of chaos in plasmas is highlighted.

Keywords. Chaos; turbulence, Alfven waves; plasma.

PACS No. 52.35

1. Introduction

The topic of my lecture, namely Chaos, is truly interdisciplinary. It occurs in a variety of physical systems e.g., astrophysics, optics, condensed matter physics, plasmas, fluids etc. and also in biological systems, chemical systems, atmospheric sciences, biophysics, ecology, neural networks etc. The mathematical techniques to study chaotic phenomena in any of these systems are the techniques of nonlinear dynamics. However, I will confine myself to plasma systems. We plan to develop the subject by trying to answer the following questions: How exactly do we define a chaotic system? How and why do we study chaos? Are there any practical applications of chaotic phenomena? Chaotic dynamics vis-a-vis turbulence?

There is no unique definition of chaos. The simplest way it can be defined is as follows: If we map the trajectory of a particle in a given field and if the trajectory is not smooth but scattered, then the system can be chaotic. The scattered mapping, in fact, is a necessary condition for the system to be chaotic. Another necessary condition for a chaotic system is its extreme sensitivity to the initial conditions; in other words the two neighboring trajectories, with very slightly different initial conditions, should diverge exponentially. For example if $|X_a(0) - X_b(0)| = \epsilon$, then $|X_a(t) - X_b(t)| = \epsilon \exp(\alpha t)$ with $\alpha > 0$, is a must for a chaotic system (a and b are two neighboring trajectories). The latter can be more rigorously defined by means of Liapunov exponent which is defined as

$$\mathcal{L} = \lim_{\tau \to \infty} \frac{1}{\tau} \frac{D(\tau)}{D(0)},$$

where D is the physical distance between two neighboring trajectories in phase space. It turns out that $\mathcal{L} > 0$, is necessary as well as sufficient condition for the system to be

chaotic. Moreover $\mathcal{L}^{-1}$ gives the characteristic time for the onset of chaos. Since $\mathcal{L} > 0$ means an inability to specify the microscopic state of the system as it evolves, one immediately starts asking the following question: Is Liapunov exponent related to the entropy in any way? The answer is yes. In fact the KS entropy $= \Sigma$ all positive $\mathcal{L}$; Kolmogorov–Sinai (KS) entropy is a measure of loss of information of a dynamical system. A word of caution may be in order here. Chaos should not be equated simply with the disorder. It is more appropriate to consider chaos as a kind of order without any periodicity. In place of periodicity, chaotic system is characterized by scale-invariance property according to which the structure of the system does not change with the changes in scaling.

Historically Jules–Henry Poincare was the first person to recognize the chaotic behaviour of a dynamical system. He encountered this unexpected behaviour in his studies of three-body problems in planetary systems. The puzzling behaviour encountered by Poincare was simply because he was dealing with nonintegrable systems. We will elaborate on the nonintegrable systems, which lead to chaos, in the next section.

1.1 *Nonintegrable systems*

A system with N degrees of freedom, if it has N independent integrals of motion, is an integrable system. This is only a necessary condition for integrability. The necessary and sufficient condition for integrability is satisfied only if N independent constants

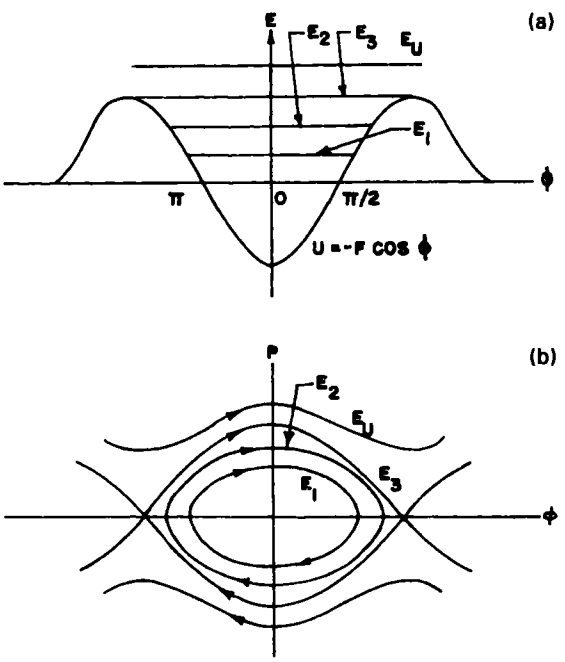

Figure 1. Energy diagram (**a**) and the corresponding phase space orbits (**b**) for an oscillator in a potential $U = -F \cos \phi$.

of motion $C_1, C_2, C_3, \ldots, C_N$ are in involution i.e., $\{C_i, C_j\} = 0$, where $\{\ \}$ represents the Poisson bracket. As a simple example, consider an oscillator moving in a potential $U = -F\cos\phi$ (cf. figure 1). The Hamiltonian for this oscillator, namely

$$H = p^2/2m + U = E,$$

has the total energy E which is conserved; this satisfies the necessary and sufficient condition for integrability. For $E < F$, the orbits are closed and for $E > F$, orbits are open but smooth. $E = E_s = F$, corresponds to the separatrix for which the period of oscillation is infinity. The two points, $\phi = \pm\pi$, where the two branches of the separatrix cross, are the hyperbolic points and the phase trajectories near these points diverge from them. Even very small perturbation in the neighborhood of the separatrix could lead an integrable system to nonintegrability. An integrable system can never lead to chaos whereas a nonintegrable system would.

1.2 *Surface of section*

Nonlinear dynamical systems are governed by nonlinear differential equations which most often can not be solved analytically. For such complex dynamical systems Poincare suggested geometrical method called surface of section. Let the phase space trajectories, of a particle or an oscillator in a given field, intersect the surface S at points $A_1, A_2, A_3, A_4, \ldots$. If the points $A_2, A_3, A_4, \ldots$ fall on A_1, then the system for sure is periodic. In case they do not fall on A_1 but the curve joining A_1, A_2, A_3 etc. is smooth, then the system is nonchaotic. On the other hand if the set of points A_1, A_2, A_3 etc. is random, the system is chaotic. We will use this technique for studying the chaotic phenomena in Hamiltonian as well as dissipative systems.

1.3 *Fractals and strange attractors*

In Hamilitonian systems, the phase space volume is conserved but in dissipative systems, the phase space shrinks continuously with increasing time; this leads to phase space of lower dimensionality and to an attractor. In case of regular motions the attractors are simple attractors e.g. a fixed point (sink) or a singly periodic orbit (limit cycle). For two-dimensional flows, sink and the limit cycle are the only two possibilities. However for three dimensional flows, one can also have doubly periodic orbits or attractors with complicated structures. Unlike the simple attractors like a point, a line etc. which have integral dimensions, attractors with complicated structures can have fractal dimensions; such attractors are known as strange attractors. Another characteristic, of strange attractors, is the scale invariance property i.e., on finer and finer scales the structure repeats itself. The attractor dimenson is defined as

$$D_a = \lim_{\epsilon \to 0} \frac{\ln n(\epsilon)}{\ln(1/\epsilon)},$$

where n is the minimum number of N-dimensional cubes of side ϵ needed to cover the basin of the attractor.

2. Nonlinear pendulum

As an illustrative example, let us consider the simplest possible nonlinear dynamical system namely a nonlinear pendulum, which is governed by the nonlinear equation

$$\frac{d^2\phi}{dt^2} + \omega_0^2 \sin\phi = 0, \tag{1}$$

with ϕ as the amplitude of the pendulum and ω_0 its angular frequency. For small ϕ, eq. (2) reduces to the equation of a simple pendulum whose solution is given by

$$\phi = a\cos(\omega_0 t) + b\sin(\omega_0 t). \tag{2}$$

Equation (2) is nonlinear but it can be solved exactly to give

$$\dot{\phi} = 2\mathcal{K}\, Cn(t;\mathcal{K}), \tag{3}$$

where Cn is the Jacobian elliptic cosine function and $\mathcal{K}^2 = (1+H)/2$ with H as the Hamiltonian corresponding to eq. (2) for $\omega_0 = 1$, i.e.

$$H = 1/2\,\dot{\phi}^2 - \cos\phi;\ \dot{\phi} = \frac{d\phi}{dt}. \tag{4}$$

The frequency of nonlinear oscillations is given by

$$(\pi/2)[1/F(\pi/2;\mathcal{K})], \tag{5}$$

where F is an elliptic integral of first kind. We may mention that the phase space diagram $(\phi, \dot{\phi})$ is identical to the one in figure 1 with $H = 1$ corresponding to the separatrix and $H < 1 (H > 1)$ leading to the trapped (untrapped) orbits.

Let us now consider a dampled nonlinear pendulum which is govened by

$$\frac{d^2\phi}{dt^2} + \sin\phi = -C\frac{d\phi}{dt}, \tag{6}$$

where C is the damping co-efficient. This damping could be due to air resistance provided by some sort of a vane attached to the swinging pendulum. The phase space diagram in this case shows a simple point attractor at $(0,0)$. If we drive this damped pendulum, say by a torque $(d\sin\phi)$, then this driven pendulum is described by the equation

$$\frac{d^2\phi}{dt^2} + C\frac{d\phi}{dt} + \sin\phi = -d\sin\phi\cos(\Omega t), \tag{7}$$

where Ω is the frequency of the driver. Numerical solution of eq. (7) shows the following interesting features [1]:

1. After the transit behaviour, the pendulum oscillates with a period which is double the period of the driver.
2. If we change the value of d slowly, for $C = 0.1$, we observe that at $d = 1.35$, there is a sudden jump in the pendulum frequency and momentarily it becomes singly periodic.
3. Further increase in $d(d > 1.35)$ leads to a sequence of period doubling bifurcations and eventually to chaos.

It is rather intriguing to find that a simple nonlinear dynamical system like a pendulum, when driven by an external torque, can become chaotic. Following the techniques used for the nonlinear pendulum, we can study the chaotic phenomena in all the other systems. We will further illustrate this by taking an example from plasmas. In this case we will also briefly discuss some applications of chaotic fields and say something about controlling the chaos.

3. Chaos in plasmas

The study of phenomena of chaos, in plasmas, is being pursued essentially to understand the phenomena of plasma turbulence which is very often observed in laboratory, space as well as in astrophysical plasmas. A chaotic system is essentially a turbulent system. As in the case of nonlinear pendulum, we have used the techniques of nonlinear dynamics to study the chaotic processes in plasmas. As an illustrative example, we will discuss chaotic Alfvén waves. Large amplitude Alfvén waves have been observed [2] in solar wind, planetary bow shocks, interplanetary shocks, environment of comets etc. Even the Alfvénic turbulence has been observed in the solar wind [3] as well as in the vicinity of comets [4].

A nonlinear wave, in general, is equivalent to a nonlinear dynamical system which exhibits the phenomena of chaos. Here we will discuss how and under what conditions, the nonlinear Alfvén waves can become chaotic; these chaotic fields in turn can lead to anomalous effects like plasma heating, particle acceleration and diffusion. These anomalous effects are essential to properly interpret some of the intriguing observations, e.g., solar coronal heating, energetic heavy ions in the vicinity of comets Halley and Giacobini-Zinner observed by recent cometary space missions [5, 6].

3.1 *Hamiltonion systems*

Let us consider a plasma which is embedded in a magnetic field $\mathbf{B}_0$ in the x–y plane. The electromagnetic waves propagating along x-direction in this plasma are governed by the two-fluid equations [7, 8]. By means of singular perturbation method, we can show that these fluid equations along with the generalized Ohm's law, lead to the following *evolution equation* for the nonlinear Alfvén waves [7, 8]:

$$\frac{\partial \mathbf{b}_\perp}{\partial t} + \alpha \frac{\partial}{\partial x}(\mathbf{b}_\perp \mid \mathbf{b}_\perp \mid^2) + \mu\left(\hat{e}_x \times \frac{\partial^2 \mathbf{b}_\perp}{\partial x^2}\right) = 0, \tag{8}$$

where $\mathbf{b}_\perp = (b_y, b_z)$, $\mu = V_A/(2\Omega_i)$, $V_A = B_0^2/4\pi\rho$ = Alfvén speed, $\Omega_i = eB_0/m_ic$ = ion cyclotron frequency, $\alpha = 1/4(1-\beta)$ with β as the plasma β i.e., the ratio of the kinetic pressure to the magnetic pressure. Equation (8) governs the elliptically polarized Alfvén waves; for circularly polarized waves this reduces to

$$\frac{\partial b_\pm}{\partial t} + \alpha \frac{\partial}{\partial x}(b_\pm \mid b_\pm \mid^2) \pm i\mu \frac{\partial^2 b_\pm}{\partial x^2} = 0, \tag{9}$$

where $b_\pm = b_y \pm ib_z$; b_+ for left hand polarized mode and b_- for right hand mode. Throughout this paper we have used the normalized units [7]. We may note that eq. (8) is

a coupled nonlinear equation whereas eq. (9) shows that left-hand and right-hand modes get decoupled. Equation (9) is the derivative nonlinear Schrödinger (DNLS) equation, which can be solved exactly; its solution is given by [9],

$$| b_+ |^2 = \pm \frac{8(1-\beta)(V-V_s)}{\sqrt{2}\cosh[2(V-V_s)(x-V_s t)] \pm 1}, \tag{10}$$

where V is the phase velocity of the linear Alfvén wave ($= V_A$ in unnormalized units) and V_s is the speed of solitary Alfvén wave. Equation (10) is the solitary wave solution for left-hand polarized Alfvén wave. Since the left-hand side of (10) is positive definite, the solution with (+) sign will correspond to

$$(1-\beta)(V-V_s) > 0$$

and the one with (−) sign to

$$(1-\beta)(V-V_s) < 0.$$

We may point out that the plasma β plays a very crucial role. For $\beta < 1$, super-Alfvénic solitons have larger amplitude compared to the amplitude of the sub-Alfvénic solitons, but for $\beta > 1$, the behaviour is reversed. It is interesting to note that for laboratory plasmas, $\beta < 1$ but for space plasmas, $\beta > 1$ for many systems.

So far, we have considered only uniform plasmas. However, very often, we encounter nonuniform plasmas. Repeating the procedure outlined above, we have derived the evolution equation for plasmas with weak but arbitrary inhomogeneity. The equation in this case is modified DNLS, which by means of a series of complicated transformations can be reduced to DNLS [10, 11]; once again we get solitary waves, which no more move with constant speed. These solitary waves get accelerated or decelerated depending on whether the wave propagation is along the increasing density gradients or decreasing density gradients. The evolution equation as well as its solutions are complicated, so they are not presented here (cf. ref. [10] and [11]).

Unlike (9), eq. (8) cannot be solved analytically. For any further analysis of eq. (8) and for investigating the possibility of chaotic behaviour of the system governed by this equation, it is useful to use the *Hamiltonian formulation.*

In a stationary frame of reference, namely,

$$\xi = (x - Vt)/\mu,$$

eq. (8) can be rewritten as

$$\hat{e}_x \times \frac{\mathrm{d}\mathbf{b}_\perp}{\mathrm{d}\xi} = \frac{\mathrm{d}\Psi}{\mathrm{d}\mathbf{b}_\perp}, \tag{11}$$

where

$$\Psi(\mathbf{b}) = \alpha\left[\frac{1}{4}(b^2 - b_0^2)^2 - \frac{\lambda b_0^2}{2}(\mathbf{b} - \mathbf{b}_0)^2\right]$$

with b_0 and λ as constants [7, 12, 13]. It is instructive to note that eq. (11) is equivalent to a classical equation of motion of a particle, with zero mass, which is moving under the influence of the coriolis force and a pseudo potential Ψ. The equipotential contours of Ψ, thus represent the trajectories of this pseudo particle with zero mass. In terms of the

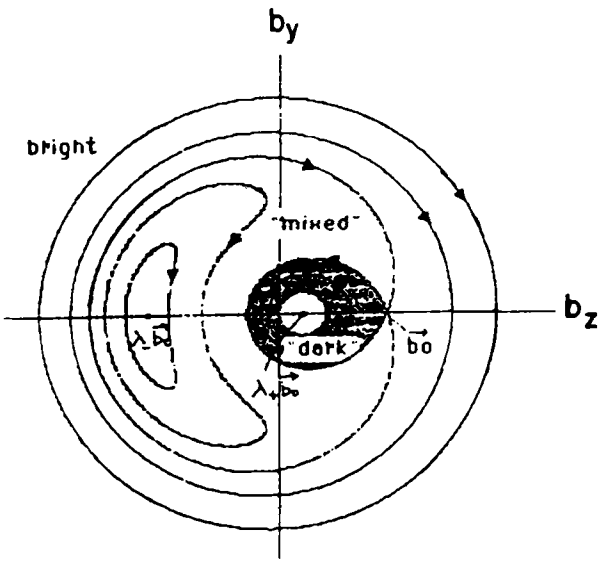

Figure 2. Equipotential contours of the pseudo potential Ψ. Also shown are 3 different solutions namely dark, bright and mixed solitons. Mixed solitons correspond to $\Psi < 0$.

Hamiltonian (H) which in this case is nothing but Ψ, eq. (11) can be represented by a set of following two equations:

$$\frac{db_y}{d\xi} = \frac{\partial H}{\partial b_z}, \tag{12a}$$

$$\frac{db_z}{d\xi} = -\frac{\partial H}{\partial b_y}. \tag{12b}$$

We immediately recognize these equations as Hamilton's equations with b_y and b_z as canonical co-ordinates. The potential Ψ being a quartic has four solutions, namely, the minimum at $(\lambda_- b_0)$, the maximum at $(\lambda_+ b_0)$ and the saddle point at b_0. For $0 < \lambda < 1/2$, $\lambda_\pm$ are given by [12],

$$\lambda_\pm \equiv \tfrac{1}{2}[-1 \pm (1 + 4\lambda)^{1/2}]. \tag{13}$$

For this range of λ, the equipotential contours of Ψ and the three solutions corresponding to dark, bright and mixed solitons are shown in figure 2. For $\beta < 1$, dark (bright) solitons have right (left) hand polarization. These solitons do not interact with each other and hence there is absolutely no possibility of having a chaos.

3.2 *Driven hamiltonian systems*

From figure 2, it is very apparent that the solitary (localized stationary nonlinear) Alfvén waves, left to themselves, will propagate as such for ever but this is somewhat an ideal situation. We would like to find out what happens to these solitary waves when there is

some local disturbance e.g., if there is a possibility of having another plasma wave generation or there is some solar activity (say a solar flare) which could propagate and interact with the Alfvén waves. To explore this, we will first consider the external driver as a plane wave. In order to make the problem tractable i.e., to be able to reduce the coupled partial differential equations (given by eq. (8)), modified by the driver, to a set of ordinary differential equations like eq. (12), we have to further restrict ourselves to the driver which is stationary in the frame of reference of the stationary Alfvén waves. This is indeed a very big restriction; in the latter part of this paper we will remove this restriction. Equation (12), in the presence of such a driver, is replaced by [7, 8],

$$\frac{\mathrm{d}b_y}{\mathrm{d}\xi} = \frac{\partial H}{\partial b_z} + A\cos\theta, \tag{14a}$$

$$\frac{\mathrm{d}b_z}{\mathrm{d}\xi} = -\frac{\partial H}{\partial b_y} + A\sin\theta, \tag{14b}$$

$$\frac{\partial\theta}{\partial\xi} = \Omega. \tag{14c}$$

In eqs (14), A is the amplitude of the driver and Ω is its frequency. We will now show that for $A \neq 0$, the dark, bright and the mixed solitons start interacting among themselves and when the driver is sufficiently strong i.e., A is sufficiently large, this interaction can lead to chaos. The reason for the appearance of chaos is rather transparent. In the absence of the driver, our system has two degrees of freedom (cf. eqs (12)) but in the presence of the driver, it has three degrees of freedom (cf. eqs (14)) and from our knowledge of nonlinear dynamics, we know that the minimum number of degrees of freedom required, for a system to be chaotic, is three and hence the possibility of chaos with the driver. For the left-hand polarized driver i.e., $\Omega = -2$, our numerical results are summarized by Poincare maps shown in figure 3. For $A = 0$, the entire set of Poincare points, originating from a given initial point, remains on the potential contour containing that initial point. For $A = 0.002$ i.e., for a weak driver, one of the sets of Poincare points, near the bright soliton separatrix, starts to scatter in a limited region of phase space. This leads to the onset of chaos for this set of Poincare points. We notice the formation of 3 islands near the local minimum of the potential Ψ. The number 3 is not a magic number; this is simply because we have taken $\omega/\Omega \sim 2/3$ (ω being the frequency of Alfvén waves). For somewhat stronger driver e.g., for $A = 0.2$, the system is almost chaotic except for the region inside the dark soliton (cf. figure 2). This region is unaffected because of the difference in polarity of the driver ($\Omega < 0$) and the Alfvén waves ($\omega > 0$). There is little interaction of the driver and the Alfvén waves because of opposite polarities. We repeated these calculations with the right hand polarized driver ($\Omega = 2$); these results are shown in figure 4. Comparison of Poincare maps for $A = 0.2$ for $\Omega < 0$ and $\Omega > 0$ testifies our above drawn conclusion. No matter how strong is the driver, the region inside the dark soliton remains coherent for $\Omega < 0$. It is this what we call 'coherence in chaos'.

3.3 *Dissipative systems*

Our entire discussion, so far, has been about the chaotic phenomena in nondissipative plasmas. Now we will very briefly present our efforts in this direction in connection with

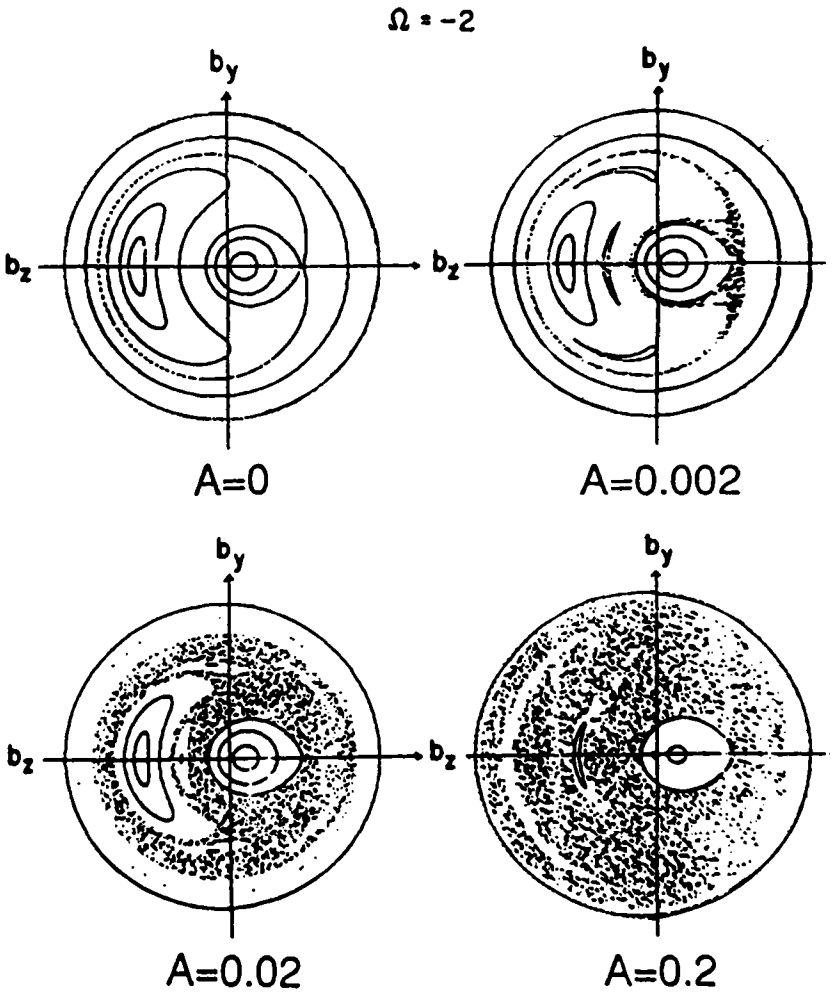

Figure 3. Poincare maps for the left hand polarized driver ($\Omega = -2$) for various amplitudes of the driver.

the dissipative systems. You notice that we had started with the simplest possible system and have been introducing the complexities into our system one by one. This step by step approach is simply to get a good physical insight into the complex phenomena of chaos.

For a dissipative two-species plasma, the nonlinear evolution equation for stationary Alfvén waves is given by [7, 13]

$$\hat{e}_x \frac{\mathrm{d}\mathbf{b}_\perp}{\mathrm{d}\xi} + \nu \frac{\mathrm{d}\mathbf{b}_\perp}{\mathrm{d}\xi} = \frac{\partial \Psi}{\partial \mathbf{b}_\perp} + A \begin{pmatrix} \cos \Omega\xi \\ \sin \Omega\xi \end{pmatrix}, \tag{15}$$

where $\nu > 0$ for dissipation and in the last term on right side of eq. (15), we have $\cos(\Omega\xi)$ for b_y and $\sin(\Omega\xi)$ for b_z component of the vector equation. Following the procedure outlined in the preceding sections, we have done the detailed analysis of eq. (15) and have

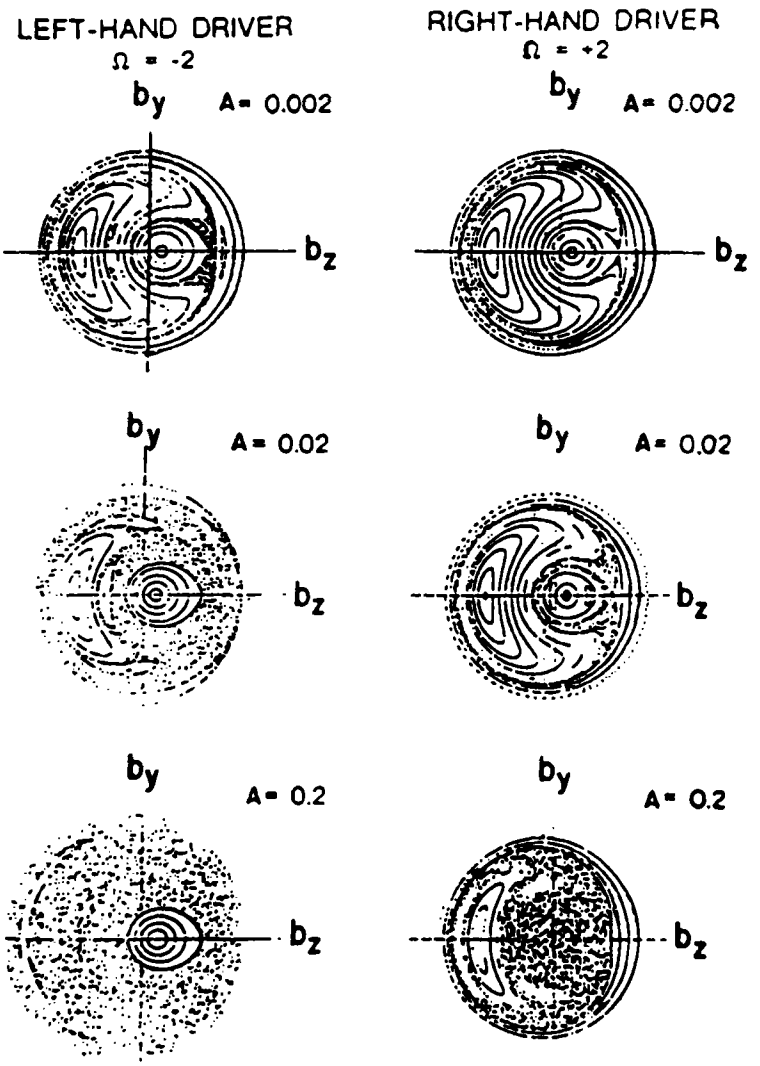

Figure 4. Comparison of Poincare maps for the left and the right hand drivers. The left hand column is the repetition of figure 3.

come up with some very interesting results. Summary of these results is presented in figures 5 and 6. Figure 5 shows the orbits as well as the Poincare points (shown by dots) in the $b_y - b_z$ phase space. The number of dots represents the periodicity. For $A = 0$, we found two attractors: one at the minimum of the potential and the other one at the saddle point. Figures 5 and 6 show the evolution of these attractors as A increases. The most interesting observation that we make is the complicated structure of the attractor for $A = 0.16$ (shown in I). In this box, we have not drawn the orbits but only the Poincare points are shown. This attractor is a strange attractor; this we have confirmed by checking its self-similar property and by determining its fractal dimension which

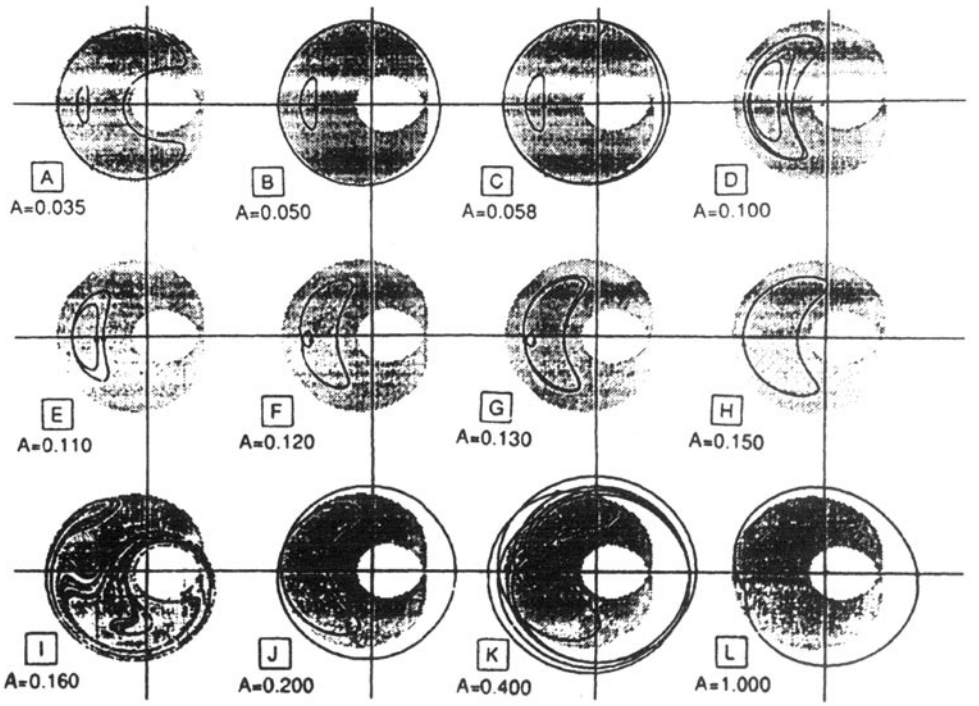

Figure 5. Shows attractors for the driven dissipative system in $b_y - b_z$ phase space. The labels are the same as in figure 6. The dots on the trajectories are the Poincare points. In (I), trajectories are omitted and only the Poincare points are plotted. The complicated structure of the attractor in this case represents a strange attractor for $A = 0.16$.

is found to be 1.57. For further discussion of figure 5, refer to Hada *et al* [13]. Another very interesting observation we make from figure 6 is that the chaos arises through two very distinct channels. At the saddle point, there are three sporadic attractors at $A \sim 0.035$, $A \sim 0.042$ and $A \sim 0.102$. The chaos in this channel arises through a sequence of period doubling bifurcations. However, at the minimum of the potential, in the region of strange attractor, there is a sudden transition to chaos. For more details, see Hada *et al* [13].

4. Control of chaos

So far our discussion has been confined to plasmas with only two species e.g., hydrogen plasma. Very often, we encounter multispecies plasmas with electrons, protons and heavy ions; the heavy ions, in laboratory plasmas, may be as impurities and in some natural plasmas as a genuine constituent, e.g., solar wind is composed of electrons, protons and α-particles (helium).

To study the chaotic processes in such multispecies plasmas, starting from the corresponding multifluid equations we derived the evolution equation [9] which is given

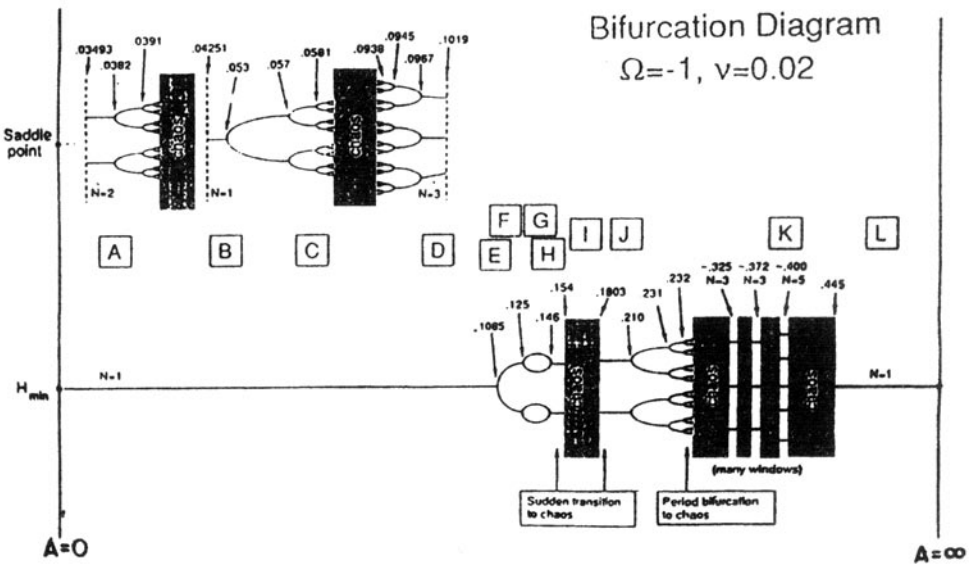

Figure 6. Shows the evolution of various attractors as the amplitude of the driver increases. The numbers on the top side correspond to the amplitudes. The top channel shows the normal as well as the reverse bifurcations. The bottom channel gives sudden transition to chaos in the neighbourhood of the strange attractor at $A = 0.16$.

by eq. (8) but with α and μ defined by

$$\alpha = \frac{1}{4}\sum_s \frac{\rho_{s0}^2(1 - Z_s\delta)}{(\rho_{s0} - \gamma_s P_s)},$$

$$\mu = \frac{1}{2}\sum_s \frac{\rho_{s0}}{Z_s},$$

$$\delta = \sum_s \frac{\rho_{s0} Z_s \gamma_s P_s}{(\rho_{s0} - \gamma_s P_s)} \left[\sum_s \frac{Z_s^2 \rho_{s0}^2}{(\rho_{s0} - \gamma_s P_s)}\right]^{-1}.$$

For solar wind parameters with 5% helium in abundance, we repeated our calculations; Poincare maps, for the two-species and the three-species plasmas, are shown in figures 7 and 8 respectively [14]. For both the figures, the driver is the left hand driver. Since all the parameters for both the figures are the same, figure 8 shows the effect of α particles. From comparison of these two figures, it is evident that the chaos is reduced due to the presence of helium–in other words, the threshold for chaos goes up because of heavy ions. Physically this could be interpreted as the inertial stabilization due to heavy ions.

5. Anomalous heating and particle acceleration

Chaotic systems can be very efficient sources of particle acceleration and plasma heating [15, 16, 17]. Lakhina and Buti have shown that the pick-up cometary ions [15] as well as the hot electrons injected from the solar coronal loops [17] can lead to unstable lower-

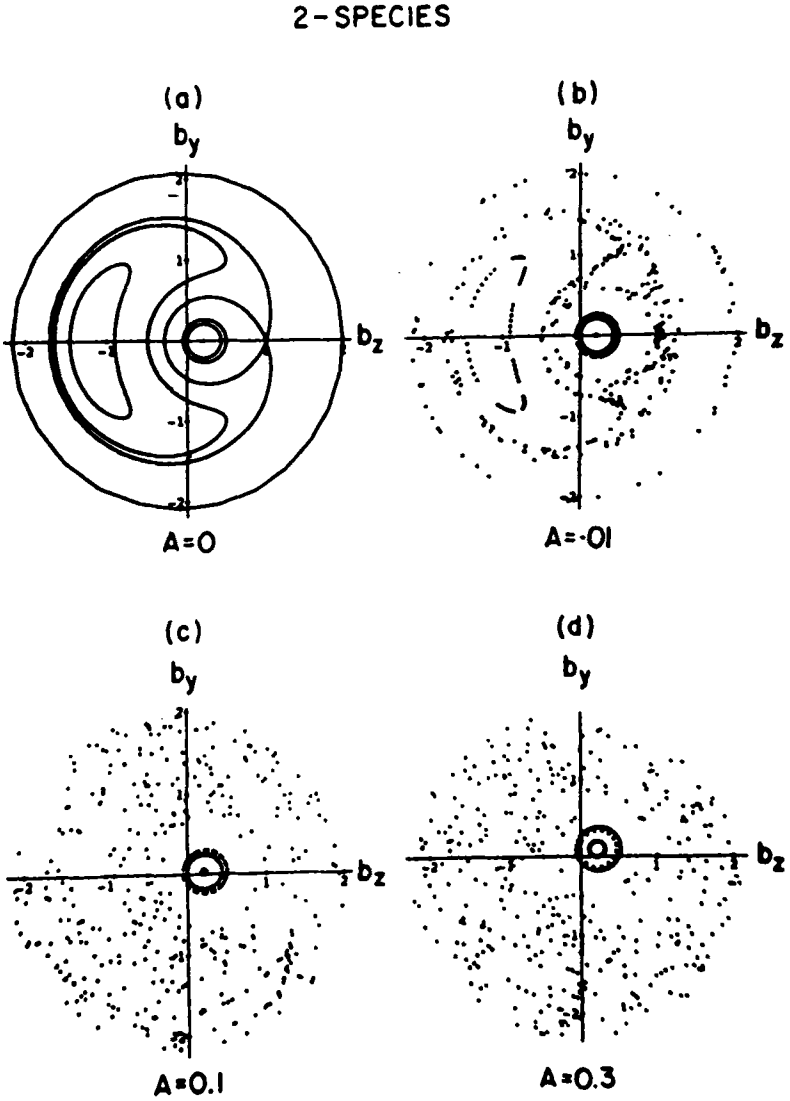

Figure 7. Poincare maps for driven Hamiltonian system for solar wind at 1 AU with only two species (electrons and protons). Driver in this case is left hand polarized.

hybrid waves. The saturated electric fields associated with these lower-hybrid waves, in both the cases, exceed the threshold for the generation of chaotic fields. They also showed that these chaotic fields preferentially accelerate the heavier ions. The maximum energy gained by the particles, from the chaotic fields, is proportional to the 5/3rd power of the mass of the particle. A part of the maximum energy gained is utilized in anomously heating the plasmas. We are now investigating the contributions of chaotic Alfvén waves, discussed in this paper, towards the anomalous heating of solar corona and anomalous acceleration of cometary ions. These will be reported in a forthcoming paper.

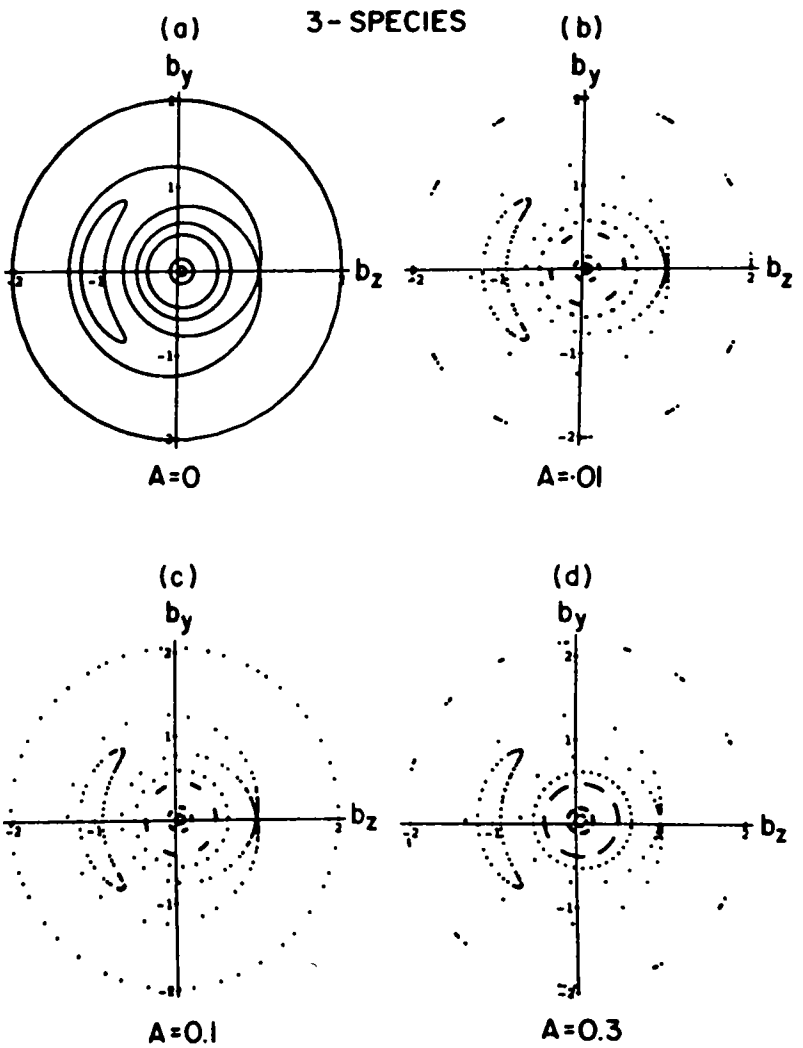

Figure 8. Same as figure 7 but for solar wind with three species i.e., electrons, protons and α particles; $N_\alpha/N_p = 0.05$. This figure is also valid for cometary plasma with water group ions as the third species and with $N_i/N_p = 0.01$ and $m_i/m_p = 16.8$ (i represents heavy ions and p represents protons).

6. Conclusions

The techniques, used in this paper for the study of chaotic Alfvén waves, can be used for the study of chaotic phenomena in any other system. Here we have discussed only the stationary waves with a very special kind of driver. However, this restriction on the driver can be relaxed; we can consider any other driver e.g., a beam representing solar wind or a pulse representing solar burst or a wave packet or any other type but then we cannot reduce our partial differential equation (cf. eq. (8)) to ordinary differential equations and

we have to solve partial differential equations. We now have a code for solving PDEs; this solution gives us the time series (time evolution) for b_y and b_z. From the time series, like in the case of observed time series, we have calculated the energy spectrum, correlation dimension and Lyapunov exponents which characterize the phenomena of chaos [18]. The latter calculations for a variety of drivers are under progress. The different spectra obtained for different drivers will be compared with the observed spectrum to finally conclude about the source of observed Alfvénic turbulence. As mentioned earlier, here we have considered Alfvén waves but the procedures outlined here are applicable to any other mode.

Acknowledgement

I would like to express my gratitude to all my collaborators of the contributions presented in this lecture.

References

[1] L Marvin and DeJong, *Phys. Teacher* **30**, 115 (1992)
[2] F L Scarf, F V Coroniti, C F Kennel, D A Gurnett and E J Smith, *Science* **232**, 382 (1986)
[3] L F Burlaga, *Rev. Geophys. Space Phys.* **21**, 363 (1983)
[4] B T Tsurutani and E J Smith, *Geophys. Res. Lett.* **13**, 259 (1986)
[5] S McKenna-Lawlor, E Kirsch, D O'Sullivan, A Thompson and K P Wentzel, *Nature (London)* **321**, 299 (1986)
[6] R J Hynds, S W H Cowley, T R Sanderson, K P Wentzel and J J Rooijen, *Science* **232**, 361 (1986)
[7] B Buti, *Solar and Planetary Plasma Physics* edited by B Buti (World Scientific, Singapore, 1990) 92
[8] C F Kennel, B Buti, T Hada and R Pellat, *Phys. Fluids* **31**, 1949 (1988)
[9] F Verheest and B Buti, *J. Plasma Phys.* **47**, 15 (1992)
[10] B Buti, *Geophys. Res. Lett.* **18**, 809 (1991)
[11] B Buti, *J. Plasma Phys.* **47**, 39 (1992)
[12] T Hada, C F Kennel and B Buti, *J. Geophys. Res.* **94**, 65 (1989)
[13] T Hada, C F Kennel, B Buti and E Mjolhus, *Phys. Fluids* **B2**, 2581 (1990)
[14] B Buti, *J. Geophys. Res.* **97**, 4229 (1992)
[15] B Buti and G S Lakhina, *Geophys. Res. Lett.* **14**, 107 (1987)
[16] B Buti, *Cometary and Solar Plasma Physics* edited by B Buti (World Scientific, Singapore, 1988) 221
[17] G S Lakhina and B Buti, *Solar Phys.* submitted (1995)
[18] L Nocera and B Buti, *Proceedings of ICPP 94* (1995)